Hindawi
Advances in Materials Science and Engineering
Volume 2019, Article ID 4985395, 13 pages
https://doi.org/10.1155/2019/4985395

Research Article

Examining the Effect of Alignment of the Rotor of the Emissions Exhaust Fan on Its Operating Parameters

Imrich Vojtko, Petr Baron, Martin Pollák, and Jakub Kaščak

Faculty of Manufacturing Technologies with a Seat in Presov, Technical University of Košice, Košice, Slovakia

Correspondence should be addressed to Petr Baron; petr.baron@tuke.sk

Received 2 November 2018; Accepted 2 January 2019; Published 21 January 2019

Academic Editor: Dimitrios E. Manolakos

The paper describes research examining the trends in balancing rotary machines and the application of the sequence of steps in execution of the operational balancing of an impeller of the industrial furnace emissions fan. The balancing process is based on the correction of the weight distribution of the body with the given axis of rotation. In trial operation, vibrations (with the measurement of the oscillation phase) were measured on both emission fan rotor bearings. Since the measured vibration value was higher than recommended, it was necessary to take steps to balance the fan's impeller. The first step of the operational balancing is to identify the initial vibration vector relative to the reference mark, arbitrarily located on the rotating wheel of the fan. In trial operation, the balancing weight mass was changed in the selected balancing level, resulting in the change of the vibration vector compared to the initial state. The size and the angular position of the balancing weight were determined from the vibration values measured. 15 months into operation after the impeller was balanced, the diagnosis of its current technical condition was performed. Total vibrations of the device were measured in the low- and high-frequency range, at four measuring points on the rotor and the drive engine. The measurement confirmed a satisfactory technical condition of the engine and the fan equipment. The effect of balancing has also been demonstrated in the case observed. Reduced bearing wear, elimination of recurrent defects, foundation damage, etc., have been observed.

1. Introduction

Vibration of working machinery and equipment has always been an unpleasant aspect of their work. Today's pressure on "greener" behaviour with less vibrating machines that would have a longer life and would be more user-friendly to operate requires addressing often complicated dynamic problems.

Imbalance and its elimination rank currently among ubiquitous, pressing problems. As a result of imbalance, the service life of machines in production is reduced, the cost of operation increases, and so does the cost of replacement of faulty parts due to uneven running of the machines. For example, an unbalanced impeller may compromise vehicle safety and increase the cost of its operation. Also, efforts by companies to progressively reduce costs and increase production by increasing production volumes, often at the expense of overrunning the machine load allowances, significantly increase the importance of the need for balancing. This is precisely why eliminating imbalance receives a great deal of emphasis especially where complex equipment with interdependent parts is concerned and where a single failure may cause a breakdown of the entire plant, halting the production and, consequently, incurring significant economic losses.

Currently, the imbalance is diagnosed, and its elimination is done using complex instruments and devices. Probably, the most widespread instruments for balancing impellers are used in tire garages, the so-called balancers. These diagnostic devices require special software to work, communicating with the operators, handling input/output data, and making individual computations.

2. Literature Review

The basic objective of observing and measuring vibrations of rotating machines is to obtain data about the rotating machine's technical condition, which can then be used to

diagnose machine failures and faults, and possibly also to ensure early repair in order to extend the service life and increase the reliability of the technical system. An integral part of fault diagnostics is evaluation of the machine condition and of the vibrations generated in the course of machine operation. The vibrodiagnostics ensures that the maintenance and repair of the diagnosed equipment is planned according to the actual condition thereof. There is a connection between the rotating machine vibrations and dynamic stress in important parts of the equipment such as bearings, gears, and other machine components. Other reasons for the occurrence of unwelcome vibrations in rotating machines are imbalance, axial misalignment, or possible damage, cracks, and wear of the machine's functional parts. Continuous monitoring and subsequent evaluation of the data obtained form the basis of technical troubleshooting.

As the vibration signal processing methods gradually developed, stationary signal analysis was based on approaches such as Fourier transformation (FT), fast Fourier transformation (FFT), and short-term Fourier transformation (STFT) [1–3]. The Fourier transformation technique has found a considerable room for application in the process of signal analysis.

However, there are some limitations to its application. Methods based on the FT are not suitable for nonstationary signal analysis [4, 5]. The signal generated by the system under observation must be linear and temporarily stationary. Otherwise, the resulting Fourier spectrum would be of only a little importance. However, in the field of technical troubleshooting performed on equipment and machines, it is necessary to analyze signals that are often nonstationary and nonlinear [3].

To analyze these signals, several new methods have recently been proposed. One such promising method is the Hilbert–Huang transformation (HHT).

HHT decomposes the signal into its own modal functions (IMF, intrinsic mode functions), which are, unlike the predefined functions used for signal decomposition by matching pursuit (MP) and wavelet transformation (WT) methods, defined by the signal itself. HHT continues to transform the original signal into an analytical signal from which immediate signal properties (instantaneous frequency, amplitude, and phase) can be obtained. These properties are the basic signs used to detect the event-related potential (ERP) of the components. There are two aspects of the method, namely, the empirical mode decomposition (EMD) and Hilbert spectral analysis (HAS). With EMD, the original signal is decomposed into a set of intrinsic mode functions (IMFs) and the signal remnant. Since applying the process of HHT is not computational intensive, the HHT becomes a promising method to extract the properties of nonlinear and nonstationary signal [3].

Bendjama et al. applied the WT to monitor the technical condition of rotating machinery [6]. The WT offers a good time and frequency localization, necessary for extraction of symptoms and for the subsequent ERP detection. The WT can be used for processing both, the continuous (CWT) and the discrete signal (DWT). The basic idea of the WT is to divide the time function into the so-called wavelet constituents. The main stimulus for development of wavelets and many related ideas was the search for fast algorithms for calculating compact representation functions and data files. The case of wavelet analysis (decomposition) of the signal, coupled with the wavelet magnitude and band, is capable of detecting the difference in signal properties at different ranges and employing the shift, and it is possible to repeatedly analyze the signal properties at various points throughout the entire range investigated. Due to, in particular, completeness of this system, it is possible to carry out a restoration (reconstruction or synthesis) of the signal via backward WT. Many studies present the applications of WT to decompose signals for improving the performance of fault detection and diagnosis in rotating machinery [7–10].

Currently, the method of time-frequency analysis is very often applied to signal processing. However, most of the existing time-frequency analysis methods decompose the signal based on a priori bases with assumption of the stationary signal. In contrast, wavelet transform and empirical mode decomposition (EMD) have effectively performed high resolution in both time and frequency domains, which have been successfully applied in faulty signal analysis. Continuous wavelet transform coefficients were used as features for the fault diagnosis system [11, 12].

Currently, artificial intelligence tools are more often used to analyze the signals obtained with vibration analysis process. Ben Ali et al. in their article [13] describe the application of the EMD method in conjunction with the use of an artificial neural network in classification of bearing defects and operational condition monitoring of rolling bearings in the process of technical diagnostics. Similarly, Castelino et al. in their scientific work applied artificial neural network tools for the vibration analysis process where discrete wavelet transform (DWT) has been used for analysis results. The statistical features have been extracted from raw vibration signal using DWT, where extracted statistical aspects were used as inputs to the artificial neural network classifier [14]. Gai and Hu have published a method based on singular value decomposition (SVD), and the fuzzy neural network (FNN) was proposed to extract and diagnose the fault features of the diesel engine [15].

Within the development of technology, full automation of production and services is more often being considered, which is in line with the approach defined as the INDUSTRY 4. Generally speaking, technology starts to replace and facilitate human work in less-qualified routine tasks. This process also concerns the area of vibration diagnostics. However, the state of artificial intelligence application in this area is not yet at a level to fully replace a diagnostician in the process- and result-based decision making of frequency spectrum analysis. Despite its considerable progress in the field of diagnostics, its use is still in automated data collection and implementation of online diagnostic systems.

3. Balancing of Rotating Parts of Machines

3.1. Machine Imbalance. Machine rotor imbalance is understood as the condition under which the residual imbalance

or oscillation of the bearing studs at operating speeds is outside the specified limits. Its main central axis of inertia is generally not identical with the rotor's axis of rotation.

Imbalance occurs due to inaccuracies in the manufacture and assembly of rotor parts or it occurs during operation.

Unbalanced rotor parts are the source of centrifugal, rotor-speed driving forces that are demonstrated as vibrations and noise.

Rotor imbalance causes the following:

(i) Increased dynamic strain of the rotor

(ii) Reduced bearing life

(iii) May cause the rotor parts to touch the stator

(iv) Caused the machine anchor system to loosen or get damaged

There are four types of imbalance as follows:

(a) *Static imbalance*. The main central axis of the rotor inertia is parallel to the rotor axis

(b) *Quasi-static imbalance*. The main central axis of the rotor inertia is independent of the rotor axis and does not pass through its centre of gravity

(c) *Pair imbalance*. The main central axis of the rotor inertia is independent of the rotor axis and passes through its centre of gravity

(d) *Dynamic imbalance*. The main central axis of the rotor inertia is offset with respect to the rotor axis [16]

3.2. Diagnostic Symptoms of Imbalance. Imbalance of rotating parts of the machine is relatively easy to diagnose, but some diagnostic symptoms are different for each type of imbalance. Basic common diagnostic symptoms of imbalance are as follows:

(i) In the frequency spectrum of radial vibrations, vibrations at the rotational frequency are dominant

(ii) The amplitude of the radial vibration vector at the rotational frequency is approximately the same in the horizontal and vertical plane

(iii) The phase shift between the radial vibration vectors at the rotational frequency in the horizontal and vertical planes is approximately 90° (±30°)

(iv) The amplitude of the vibrations increases approximately with the second power of revolutions

(v) The phase difference of radial vibration vectors at the rotational frequency on both bearings of the rigid rotor machine is approximately the same (±30°) in the horizontal and vertical planes

(vi) The phase difference of radial vibration vectors at the rotational frequency on the inner (outer) bearings (relative to the coupling) of the device is approximately the same (±30°) in the horizontal and vertical plane

The following diagnostic symptoms are yet typical for each type of imbalance:

(a) Static Imbalance:

(i) Vibrations in the radial direction are substantially higher than in the axial direction

(ii) The phase difference of radial vibration vectors at the rotational frequency on both bearings of the machine is approximately equal to 0° (±30°) in the horizontal and vertical planes

(b) Pair Imbalance:

(i) The phase difference of radial vibration vectors at the rotational frequency on both bearings of the machine is approximately 180° (±30°) in the horizontal and vertical planes

(ii) Significant pair imbalance sometimes generates high vibrations in the axial direction [16–18]

3.3. General Principles for Rotor Balancing. When balancing the rotor, it is desirable to minimize dynamic forces transmitted to the machine from its rotor by aligning the main central axis of the rotor inertia with its axis of rotation. This is accomplished by adding, removing, or displacing the correction matter in one, two, or more balancing planes.

According to the number of balancing planes and the possibility of eliminating a certain type of imbalance, two basic balancing procedures are distinguished:

(i) *Static balancing*. Balancing in one plane

(ii) *Dynamic balancing*. Balancing in two or more planes—all kinds of imbalances can be eliminated [19]

According to the rotor balancing method, three balancing modes are distinguished:

(i) Balancing on gravity-balancing devices by weighing or swinging the rotor. Only static rotor balancing can be performed in this way.

(ii) Balancing on centrifugal-balancing machines during rotation. Static and dynamic rotor balancing can be performed in this way.

(iii) Operational balancing in its own frame and its own bearings. Static and dynamic rotor balancing can be performed in this way.

During operational balancing, machine vibrations are measured, such as its response to dynamic forces transmitted from the rotor. In measuring these vibrations, the amplitude and vibration phase of the vibration vector are generally measured, while it is not critical which vibration variable (deflection, velocity, and acceleration) is measured.

The result of the operational rotor balancing process is relatively largely influenced by the size and location of the test matter during the test run of the machine. In determining the weight of the test matter, it is assumed that its mass should cause a centrifugal force equal to one tenth of the force of strain acting from the rotor to the bearing. When placing the test matter in the balancing plane, it is desirable that the matter is not placed into the "hard" point of the rotor. However, establishing this point is a problem, as normal measurements fail to identify it unequivocally.

The final criterion of the correctness of the weight of the test matter and its placement is, in particular, a sufficient change in the phase of the vibration vector in the next test run of the machine. This change should be at least 25° to 30°. Changing the vibration amplitude is not so critical but changing it by at least 30% will increase the quality of the balancing process [16].

Under real-world operating conditions, the alignment tolerance for rotating machines depends on a number of factors (operating speed, efficiency, clutch type, length of the inserted shaft, life of the technical equipment, and type of equipment). Under practical circumstances, it is problematic to consider all the influences—a certain simplification is applied, expressed in the form of recommended values of alignment tolerances (Table 1).

Table 1: Recommended alignment tolerances [21].

rpm	Angular misalignment of axes (mm/100 mm)		Parallel misalignment of axes (mm)	
	Optimal value	Limit value	Optimal value	Limit value
0–1000	0.06	0.10	0.07	0.13
1000–2000	0.05	0.08	0.05	0.10
2000–3000	0.04	0.07	0.03	0.07
3000–4000	0.03	0.06	0.02	0.04
4000–5000	0.02	0.05	0.01	0.03
5000–6000	0.01	0.04	>0.01	>0.03

3.4. Operational Balancing Methods

3.4.1. Methods without Phase Measurement. This method does not measure the phase, but overall vibrations. Here, a three-position balancing method and a multiposition balancing method that we can use for manual measurement without a balancer are applied [16].

Multiposition Balancing Method. This method requires that the rotor circumference in the balancing plane be divided into at least five equal parts (preferably 8 parts). Before balancing, the vibration of the bearing stand must be measured. To calculate the weight of the auxiliary load, the following relationship is applied:

$$m_p = \frac{m \cdot |X_A|}{r_p}, \quad (1)$$

where m_p is the weight of the auxiliary load (kg·10^{-3}), m is the weight of the rotating part (impeller, shaft, and clutch), X_A is the vibration velocity amplitude (RMS), and r_p is the auxiliary load radius, distance of its centre of gravity from the axis of rotation.

After calculating the weight of the load, it is placed in all positions, and the vibration of the bearing stand is then measured. A graph of dependence of the measured kinematic quantity on the load position is made (Figure 1). The position of the final load is subtracted from the graph, and its weight is determined by calculation. The final load is placed on the rotor, and the test is performed [16].

In case, the following relationship applies

$$X_A \geq \frac{1}{2}(X_{max} + X_{min}), \quad (2)$$

the weight of the final load is calculated according to the following relationship:

$$m_v = \frac{X_{max} + X_{min}}{X_{max} - X_{min}}. \quad (3)$$

Otherwise, if

$$X_A < \frac{1}{2}(X_{max} + X_{min}), \quad (4)$$

the weight of the final load is calculated according to the following relationship

$$m_v = \frac{X_{max} - X_{min}}{X_{max} + X_{min}}. \quad (5)$$

3.4.2. Balancing Methods with Phase Measurement. Single-Positional Balancing Method. This is the simplest method compared to other balancing methods. In this method, the oscillation phase must be measured (optical marks and optical probes are used, or the rotor is illuminated with a stroboscopic lamp synchronized with the nonweight balance vector).

When the rotor is spun, the amplitudes and the oscillation phase of the bearing stand are measured. The amplitude X_0 and the phase ϕ_0 of the oscillation deflections are measured at point A (Figure 2). The test load is then placed in a selected position of m_p weight, and at the same revolutions as in the previous case, the amplitude X_{01} and the oscillation phase ϕ_{01} of the oscillation deflections are measured at point A.

The evaluation of the measurement is performed by plotting the oscillation vectors from the two measurements in a polar diagram at the selected scale (Figure 2). *Difference of Vectors.* $X_{01} - X_0$ determines the vector coefficient α. The angle ψ, by which this vector had to rotate to merge with the vector $X_{0,}$ but with an opposite meaning, indicates the position of the desired load on the rotor relative to the position where the auxiliary load was added. The weight of the desired load is established from the following relationship:

$$m_v = \frac{X_0}{\alpha} m_p \frac{r_p}{r_v}, \quad (6)$$

where m_v is the final load weight, m_p is the test load weight, X_0 is the amplitude of the oscillation deflection at point A, α is the vector coefficient, r_p is the auxiliary load radius, distance of its centre of gravity from the axis of rotation, and r_v is the final load radius, the distance of its centre of gravity from the axis of rotation.

After the weight is calculated, the load is placed at the specified position and the test run of the rotor is performed [16, 20].

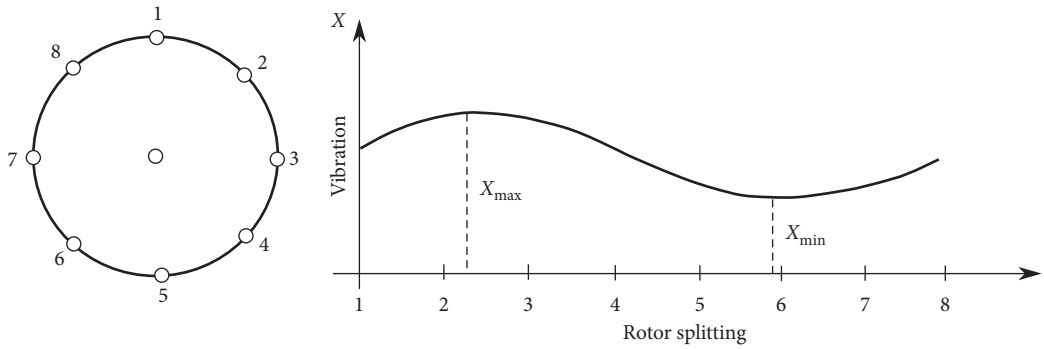

Figure 1: A multipositional balancing method graph [16].

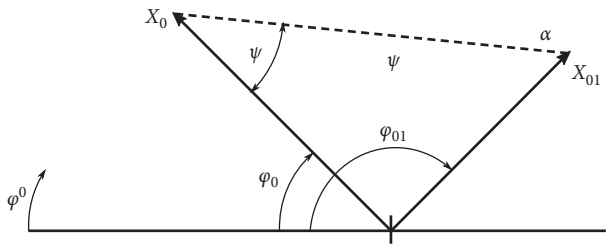

Figure 2: Principle of a single-positional method.

3.5. Balancing Rigid Rotors. The rigid rotor can be balanced even at low speeds, but it does not need to be balanced at operating speeds. The rigid rotor does not deform during rotation, its axis does not change until the maximum operating speed is reached. When balancing such rotors, the vibrations are measured in bearing bays in the radial direction where the machine must have reached operating speeds. Operating balance procedure for amplitude measurement and vibration vector phase:

(1) Basic machine run and amplitude measurement and vibration vector phase at rpm
(2) Placement of test load
(3) Test run of the machine and measurement of the amplitude and phase of the vibration vector at the rotational frequency
(4) Establishment of the load size and placement through a graph or through computation
(5) Test run of the machine with test load
(6) If the imbalance is still large, the size and placement of the additional balancing matter is calculated, but the original load remains in place [20]

In general, the greater the weight of the rotor, the greater the imbalance under the same conditions.

In calculating the permissible residual imbalance, we draw the following equation:

$$\varepsilon_p = \frac{N_p}{M}, \tag{7}$$

where ε_p is the specific residual imbalance (μm), N_P is the permissible load (g·mm), and M is the weight of the balanced tool (kg).

An important parameter in determining the permissible imbalance is the operating speed of the rotor. The degree of admissible imbalance is calculated from the following equation:

$$Q = \varepsilon_p \cdot \omega \cdot 10^{-3} = \text{const.}, \tag{8}$$

where Q is the permissible residual imbalance (mm·s^{-1}), ε_p is the specific residual imbalance (μm), and ω is the angular velocity (rad·s^{-1}).

Eccentricity of imbalance is calculated from equation (9); that is, when the value decreases, the centre of gravity approaches the axis of rotation [21, 22].

$$e = \frac{U}{M} = \frac{m \cdot r}{M}, \tag{9}$$

where e is the permissible residual eccentricity (μm), U is the permissible residual imbalance (g·mm), M is the weight of the balanced tool (kg), m is the permissible residual weight of the imbalance (g), and r is the position radius of residual imbalance (mm).

4. Analysis of the Operating Condition of the Furnace Exhaust Fan Depending on Its Impeller Alignment

Based on the requirement of our partner in the metallurgical industry, we performed a balancing of the furnace exhaust fan impeller with a diameter of 1.5 m. The impeller is fitted with eight 20 cm-wide blades. The fan is connected by means of a disc clutch to an electric motor with a power of 45 kW and a speed of 1500 rpm (Figures 3 and 4).

The measurement was carried out as follows:

Dynamic balancing of the fan impeller was performed using the Microlog CMVA 10 frequency analyser. The assessment of the fan's operating condition was carried out by measuring and evaluating vibration frequency spectra. In the test operation, vibrations were measured on both bearings (Figure 5), including the phase. Since the measured vibration value was higher than recommended, it was necessary to balance the machine.

Table 2 lists the recommended values for mechanical vibration measurements, in accordance with the ISO 10816-3 standard.

Figure 3: Placement of the emissions fan.

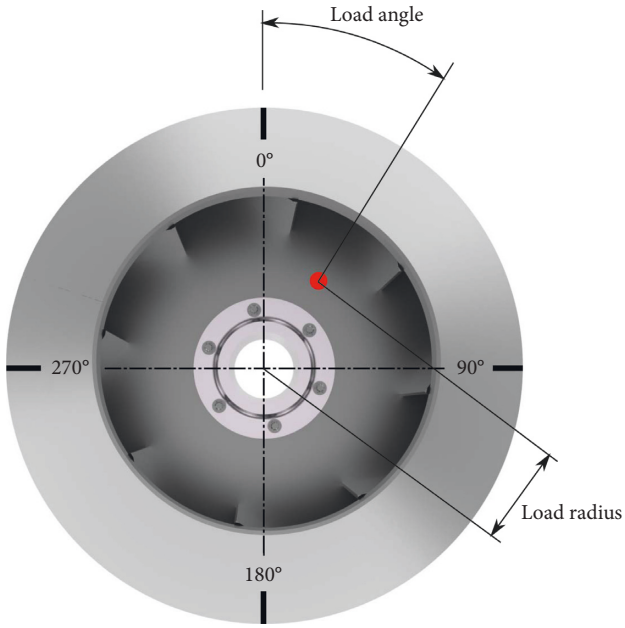

Figure 4: Splitting the rotor circumference and placing the load.

Figure 6 shows the mechanical vibrations measured before balancing at a rotational frequency of 24.5 Hz. Looking at the graph, it is possible to determine the impeller imbalance, which is at 6.9 mm·s^{-1}.

The impeller circumference has been divided into four equal parts with an angle of 90° in the direction of rotation of the fan, which is shown in (Figure 4). The first point was selected at the 30° position, where the test weights were welded.

After the load was attached by welding (Figure 7), the fan was spun to operating speeds, and vibration and phase measurements were performed on both bearings. Applying the Microlog CMVA 10 analyser, we calculated the weight of the test load and the location of its placement. The test balance load was removed with a grinder and adjusted to meet the required weight according to the respective calculation. In the next step, the load with required weight was attached by welding to the fan's circumference. A follow-up fan run was performed, in which vibrations and phases were remeasured on both bearings. The measurement results confirmed the correctness of the fan-impeller balancing procedure. The resulting impeller imbalance is 2.0 mm·s^{-1}.

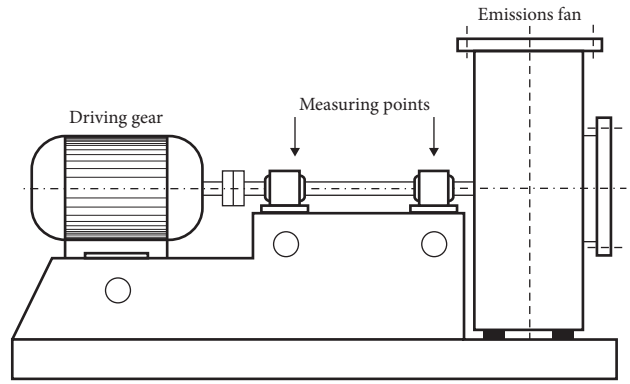

Figure 5: Scheme of the monitored device with the location of the measuring points.

Table 2: Recommended vibration values.

Measuring method	Alarm 1 (warning)	Alarm 2 (danger)
MFV (mm/s)	4.5	11.2
En3 (Eg)	4.5	11.2

The measurement results are within the limits of the recommended values given in the ISO 10816-3 (Figure 8) standard.

Table 3 shows balance load weights and position of their placement. The balance loads made of the following material were used in the structural steel EN ISO 295.

The proper machine balancing was successful. The vibration values on both bearings were below the specified limit (Table 4). The final load was firmly welded so that it does not loosen during operation, which would cause the fan impeller to resume its state of imbalance. Figure 9 shows a fan with the final balance load attached by welding.

Table 5 shows an evaluation of the operating state of the nodes of the fan measured after balancing.

At the end of the balancing process, measurements were made to determine the mechanical loosening (backlash) of the bearings at the coupling and the impeller. Figures 10 and 11 show the amplitude of the vibration signal, spectrum 3 of the envelope. It is obvious from the record that the bearings are without significant damage, but with increased radial backlash.

5. Standards for Rotor Balancing and Discussion

The results of the operational rotor balancing or balancing of a rotor assembly are evaluated according to the maximum value of the oscillating vibration variable measured at all machine-bearing supports in the vertical and horizontal directions perpendicular to the rotor axis. These measurements are performed over the full speed range, idling, and rated load.

The balancing of the rotor is considered to be completed if the maximum value of the effective oscillation velocity of the bearing supports at the idling speed does not exceed the value of the product C_0 and V_e and will not exceed the value

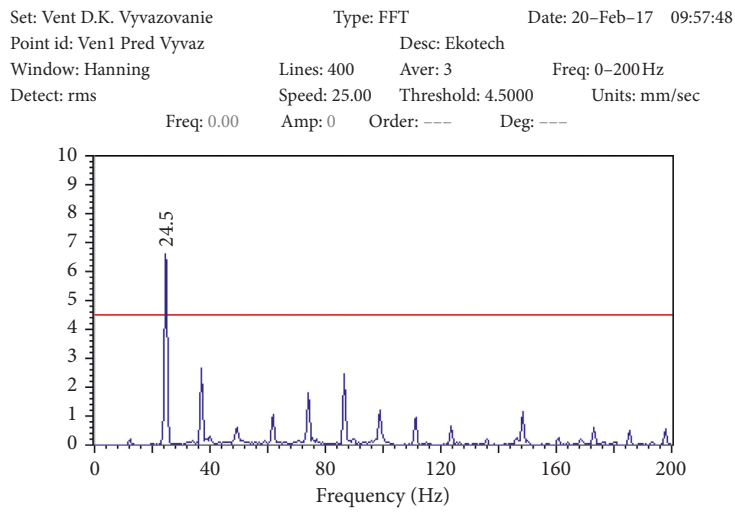

Figure 6: Condition (velocity) before balancing the fan.

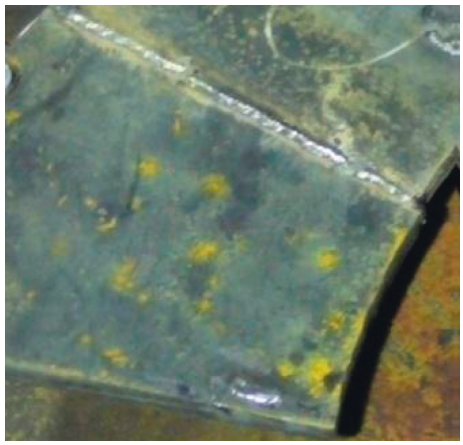

Figure 7: Applied balance load.

V_e at critical speeds, where C_0 is the ratio of the permissible value of the component of the effective oscillation velocity at the rotational frequency to the permissible total value of the effective oscillation speed of the bearing supports at the machine running under operating conditions and V_e is the permissible value of the effective oscillation speed of the bearing supports of the machine or the studs close to the bearings during operation ($mm \cdot s^{-1}$).

The quality of solid rotor balancing is evaluated on the basis of the so-called degree of balance quality Q ($mm \cdot s^{-1}$), which is defined as the product of the permissible residual specific imbalance ε_p (μm) and maximum operating angular rotation speed of the rotor ω ($rad \cdot s^{-1}$), while the permissible residual specific imbalance ε_p is defined as the portion of the permissible balance load N_p (g·mm) and the weight of the rotor M (kg) balanced.

Degrees of balance quality Q are divided into 11 classes, which then include individual types of rotating machines. Class *Q0.4* contains machines with the highest quality value of the balance (0.16 to 0.40 $mm \cdot s^{-1}$), and class *Q4000* contains machines with the lowest quality value of balance (1600 to 4000 $mm \cdot s^{-1}$).

When balancing the rotors, it is also appropriate to determine the so-called rotor sensitivity to imbalance. This parameter is easy to establish from a graph of the results of the rotor test run at operational balancing, since the sensitivity of the rotor to the imbalance is expressed as the product of the test compound test matter and the radius of its placement to the amplitude of the rotor vibration vector at the rotational frequency caused by the addition of the test matter to the rotor.

The residual imbalance of the rotor U_z (g·mm) after balancing has been performed is then determined as the product of the rotor sensitivity to imbalance and the amplitude values of the vibration vector at the rotational frequency after rotor balancing [16].

6. Verification of the Operating State of the Monitored Fan after Its Impeller Has Been Balanced

Fifteen months after the process of balancing the emissions fan impeller of an industrial furnace, our team conducted vibration measurements on the device in question to verify its current technical condition.

The total vibrations of the device in the low-frequency and high-frequency range were measured, with the measurement points according to Figure 12.

The purpose of the measurement was to investigate the total vibrations of the device. In particular, mechanical conditions, such as potential imbalance, axial misalignment, mechanical loosening, bent shaft, resonance, and transmission problems, were investigated. These measurements are defined in the standards dealing with permissible oscillation magnitudes on given devices (EN 122011: fans, EN 105041: compressors, and EN ISO 10816: general standard for most machinery). The Microlog CMVA 10 frequency analyser and accelerometer sensors of 100 mV/g were used to experimentally identify and analyze the oscillatory motion of the monitored device.

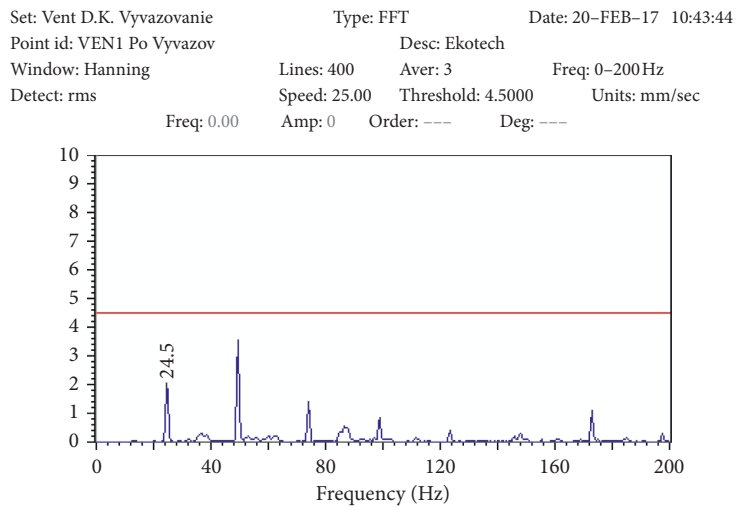

Figure 8: Condition (velocity) after balancing the impeller fan.

Table 3: Test balance load weight.

Measurement number	Balance load weight (g)	Angular position (°)
1	50	30
2	30	25

Table 4: Vibration values measured before and after balancing the fan impeller.

Fan	Mechanical vibrations at 24.5 Hz (imbalance) by MFV (mm/s)	Total mechanical vibration by MFV (mm/s)
Impeller before balancing	6.9	8.4
Impeller after balancing	2.0	4.3

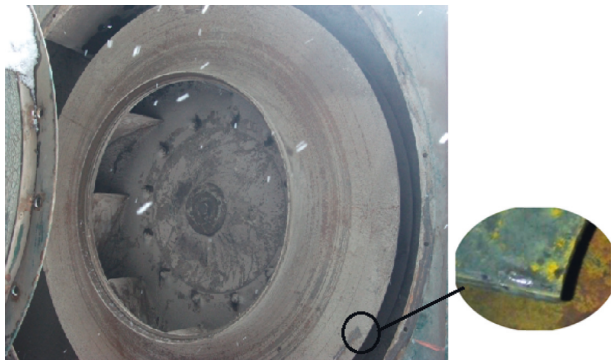

Figure 9: Aligned fan and the load detail.

To assess vibration in the low-frequency range, the following was used:

(i) Velocity measurement method (jitter speed, $mm \cdot s^{-1}$), RMS detection

Table 5: Evaluation of the operating state of the monitored fan nodes.

Machine and measuring node name	Operating state	Note
Fan engine	Satisfactory	Bearings are okay, and mechanical vibrations in the axial direction slightly increased
Fan bearings	Satisfactory	Mechanical vibrations: bearings were without significant damage but were with increased backlash

(ii) Pursuant to recommendations of ISO10816-3, the FFT spectrum for the frequency range 2–1000 Hz

(iii) Enveloping acceleration method of measurement (gE), peak detection, for the frequency range up to 1000 Hz, FFT spectrum, and time recording

For the assessment of vibration in the high-frequency range, the following was used:

(i) Acceleration (jitter acceleration) method of measurement (g), PtP detection, frequency range up to 6.4 kHz, FFT spectrum, and time recording

(ii) Enveloping acceleration method of measurement, (gE), peak detection, frequency range up to 10 kHz and up to 20 kHz, FFT spectrum, and time recording

From the point of view of the total vibration values measured, it was necessary to identify the recommended limits with respect to the requirements of the technical standard STN ISO 10816-3 [23].

For various machine-operating modes (with respect to speed, load, and power), the alarm limits (alarms) can also be determined on the basis of a general recommendation (200% signal increase over the reference value)(Tables 6 and 7).

Table 8 contains measured vibration values.

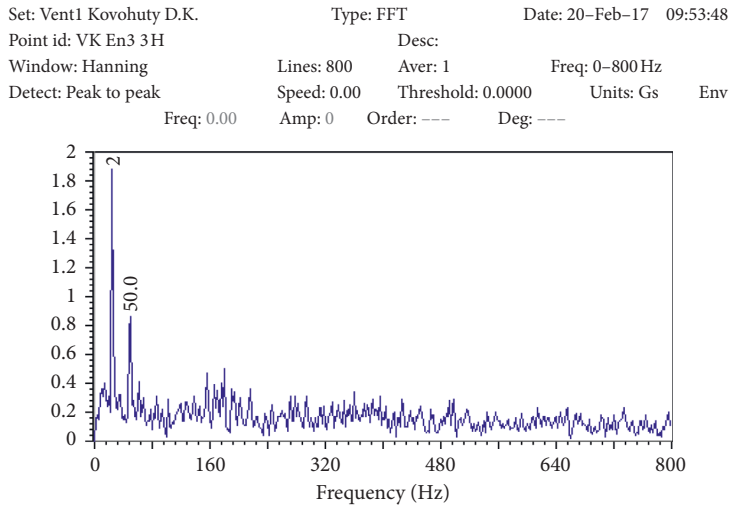

Figure 10: Bearing at coupling.

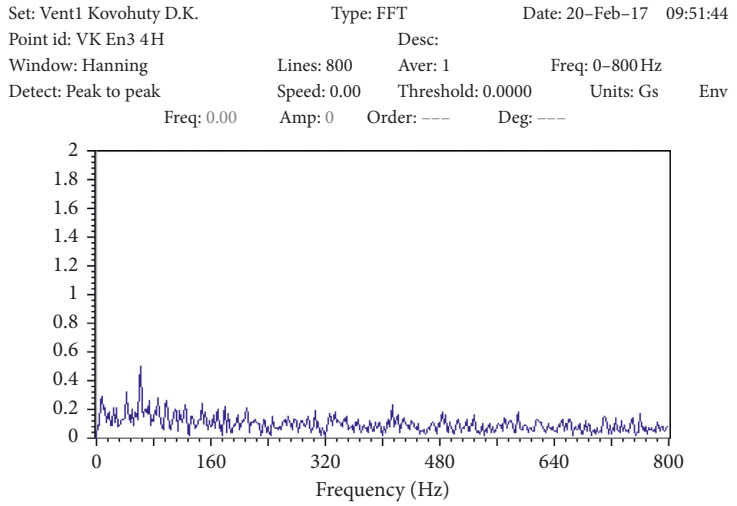

Figure 11: Bearing at the fan.

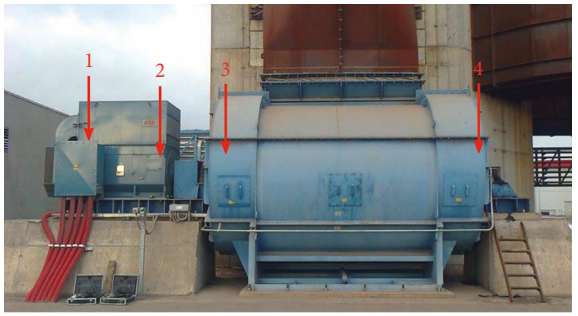

Figure 12: Location of the measuring points on the fan device.

6.1. Validation and Evaluation of Measured Data. The values measured on the engine are low in all parameters (up to 1 mm·s^{-1} or up to 1 g). LF vibrations on the impeller do not exceed the alarm value A1 (warning) either. Values measured using HF methods, however, point to a dissatisfactory operation. All values exceed A1 alarm (warning), some even alarm A2 (danger) (Table 8). Clear resonance regions are visible in acceleration spectra in the area around 3 kHz. Spectra of the 3rd envelope do not contain any dominant frequency (Figures 13–16).

Table 6: Alarm levels for LF vibration.

Alarm A1 (warning)	4.5
Alarm A2 (danger)	11.2

Table 7: Alarm levels for HF vibration.

Alarm A1 (warning)	7.1
Alarm A2 (danger)	11.2

6.2. Analysis of Measurement Results and Discussion. Based on the measurements made, it can be stated that the fan engine is in good condition and its vibrations are well below the alarm A1. The impeller is all right in terms of low frequencies (it is balanced). High-frequency vibrations at point 3 indicate bearing problems. However, the spectra do

Table 8: Vibration values measured at defined measurement points.

	Velocity (mm/s)	Acceleration (g)	En3 (gE)
Point 1H	0.70	0.41	0.55
Point 1V	0.76	—	0.49
Point 2H	0.59	0.52	0.61
Point 2V	0.82	—	0.53
Point 2A	0.31	—	—
Point 3H	1.69	**11.51**	**16.49**
Point 3V	1.00	**11.17**	**16.28**
Point 3A	0.65	—	—
Point 4H	1.83	**7.68**	**9.09**
Point 4V	1.45	**9.48**	**12.01**

not contain bearing frequencies, so it is probably not a bearing failure. We recommend the operator of the technical equipment a more frequent tracking of the bearing in point 3 (vibration, temperature, and lubrication). The bearing at point 4 was replaced, so it is possible to consider the present vibration condition on this bearing as part of the run-in process.

7. Conclusion

Dr. Jerzy Piotrowski, in his published works, states that, up to 99% of technical equipment is working with some axial misalignment. That is to say, an absolutely perfect alignment is not possible. Slight misalignment and low vibrations are, actually, often desirable to allow for functional lubrication, which is often done hydrodynamically [23]. The most important goal of alignment is to increase reliability and extend the life of the technical equipment. Efforts aiming at accurate alignment are done with the following partial goals [23–25]:

(i) Reducing excessive axial and radial forces in the bearing, resulting in increased lifetime and dynamic stability of the rotor

(ii) Avoiding damage to the shaft due to material fatigue caused by cyclical forces

(iii) Minimizing wear of the coupling part

(iv) Minimizing shaft deflection between power transmission point (for clutch) and end bearing

(v) Reduction of energy consumption (the examples shown show a saving of $2 \div 17\%$)

(vi) Reducing the vibration level of machine covers, bearing stands, and rotors

Based on the research in the field of vibrational diagnostics and rotor balancing, we can confirm the fact that the loss of balance occurring during rotation is due to uneven weight distribution that creates a centrifugal force manifested by vibrations. This centrifugal force grows quadratically with operating speed. This means that, at the same loss of balance, for example, at the operating speed of 16,000 min^{-1}, the centrifugal force affecting the rotor is 16x greater than at the operating speed of 4,000 min^{-1}.

During rotation, the unbalanced rotor tends to rotate around its central axis of mass. As the bearings limit this movement, the centrifugal force causes the rotor to vibrate due to loss of balance. These vibrations primarily cause damage to the bearings, generate excessive noise, and, in extreme cases, even lead to disintegration of the entire mechanism. Therefore, it is essential to minimize the loss of balance to an acceptable level.

Of course, development of modern production technologies has minimized the need for balancing in low-speed applications. On the other hand, dynamic balancing becomes a necessity in the application of rotary machines with growing operating speed.

Based on the analysis and monitoring of the technical system under evaluation, namely, the industrial furnace fan, the following general conclusions can be stated, equally applicable to the new rotary equipment commissioned:

(i) Although we assume that each component forming the rotary equipment was well balanced, 100 percent balance does not exist.

(ii) Although each rotating unit (engine, clutch, rotor, and fan impeller) meets the maximum criteria of residual loss of balance, the resultant loss of balance of the overall fan device driven by the electric motor may be unsatisfactory when the assembly has been completed.

(iii) Under real conditions, the position and extent of the displacement of the centre of gravity from the axis of rotation is unknown (the relative position of the rotating units is random after assembly). It is thus quite natural that the control measurements applied can identify with great probability higher vibration values than those recommended by the technical standards.

(iv) The abovementioned deficiency in both the monitored and the new rotation systems must be removed by additional balancing.

From the rotary machines' operation point of view, it is argued that the main problem of their lost balance is the occurrence of vibrations, which not only cause noise but also cause an increase in mechanical stress. Such stress is most common in bearings, which reduces their service life. The loss of balance is closely related to greater weight of the machines, and this is the reason why balancing is a necessity, especially when it comes to heavy rotating components, including the impeller of the industrial furnace fan described in the paper.

This article described the sequence of steps performed in balancing the emissions fan impeller of an industrial furnace. After addition of a balance load with weight established by calculations, a test operation of the fan was performed, with measuring vibrations and phases on both of the monitored bearings of the fan rotor. The resulting impeller imbalance reached 2.0 $\text{mm}\cdot\text{s}^{-1}$. Thus, the results of the final measurement were within the limits of the recommended values prescribed by the ISO 10816-3 standard. Verification of the technical condition of the fan rotor bearings has not shown any significant damage. Fifteen months later, upon request of our partner, we verified the actual technical condition of the emissions fan in question, with the

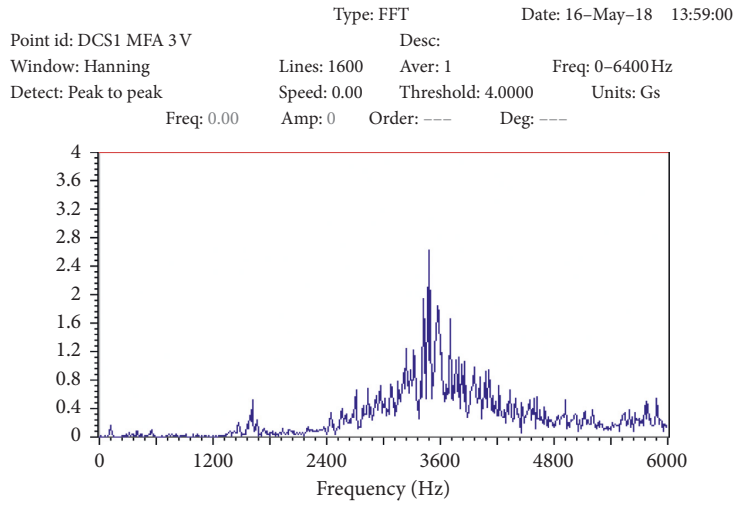

Figure 13: Jitter acceleration spectrum (Acc) at point 3 V.

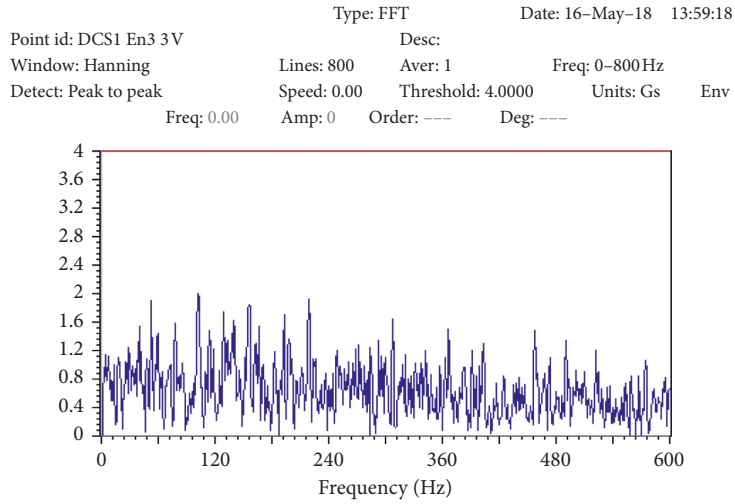

Figure 14: Spectrum of the 3rd envelope (En3) of acceleration at point 3 V.

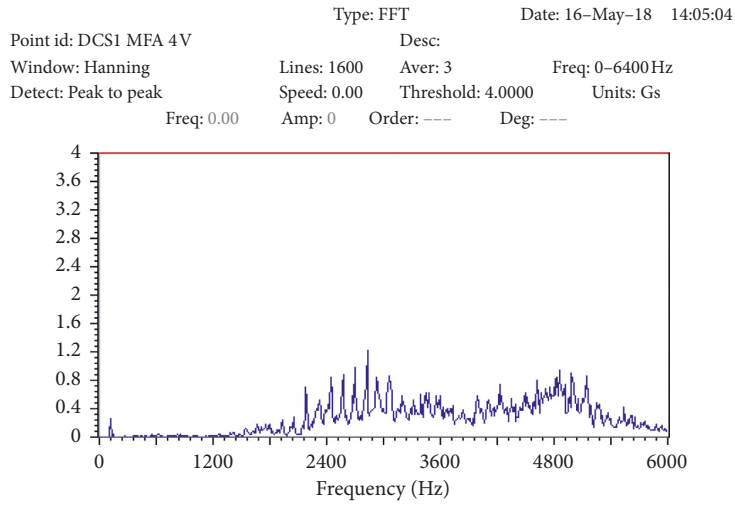

Figure 15: Jitter acceleration spectrum (Acc) at point 4 V.

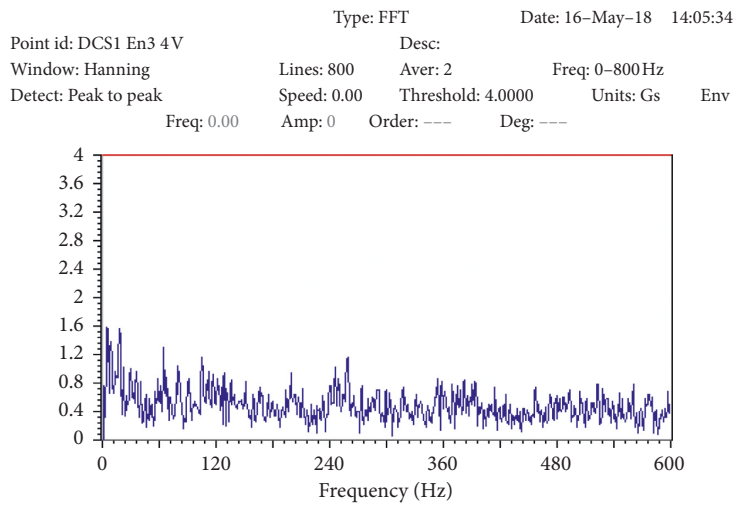

Figure 16: Spectrum of the 3rd Envelope (En3) of acceleration at point 4 V.

application of vibrodiagnostics tools. Based on the measurements made, it can be stated that the fan engine's condition is satisfactory. The impeller is all right in terms of low frequencies—it is balanced. High-frequency vibrations at measurement point 3 identified some bearing problems. However, the spectra did not contain bearing frequencies, which led to the conclusion that there was no bearing failure. We recommended the operator of the installation to track the bearing at point 3.

Our analyses, too, confirmed the connection between a reliable operation of rotary machines and the precise alignment of their rotors. Up to 50% of rotary machine failure is due to the incorrect alignment of their rotors. Device operators often rely on the clutches to bear considerable misalignment, sometimes all the way up to 10 mm of radial retraction. However, the strain on the shafts, bearings, and seals increases dramatically as a result of the increase of the alternating forces and loads [26, 27].

Data Availability

The data used to support the findings of this study are included within this article.

Conflicts of Interest

The authors declare that they have no conflicts of interest.

Acknowledgments

The authors thank the Ministry of Education of Slovak Republic for supporting this research by the grant KEGA 001TUKE-4/2018 (Implementation of concurrent engineering philosophy to educational tool in the field of computer aided technological preparation).

References

[1] K. Shibata, A. Takahashi, and T. Shirai, "Fault diagnosis of rotating machinery through visualisation of sound signals," *Mechanical Systems and Signal Processing*, vol. 14, no. 2, pp. 229–241, 2000.

[2] S. Seker and E. Ayaz, "A study of condition monitoring for induction motors under accelerated aging process," *IEEE Power Engineering Review*, vol. 22, no. 7, pp. 35–37, 2002.

[3] Z. K. Peng, P. W. Tse, and F. L. Chu, "An improved Hilbert-Huang transform and its application in vibration signal analysis," *Journal of Sound and Vibration*, vol. 286, no. 1-2, pp. 187–205, 2005.

[4] N. E. Huang, Z. Shen, S. R. Long et al., "The empirical mode decomposition and the Hilbert spectrum for nonlinear and non-stationary time series analysis," in *Proceedings of the Royal Society of London. Series A: Mathematical, Physical and Engineering Sciences*, vol. 454, pp. 903–995, no. 1971, Seattle, WA, USA, 1998.

[5] J. C. Cexus, *Analyse des signaux non-stationnaires par transformation de huang, opérateur de teager-kaiser, et transformation de Huang-Teager (THT)*, Ph.D. thesis, Université de Rennes, Rennes, France, 2005.

[6] H. Bendjama, S. Bouhouche, and M. S. Boucherit, "Application of wavelet transform for fault diagnosis in rotating machinery," *International Journal of Machine Learning and Computing*, vol. 2, no. 1, pp. 82–87, 2012.

[7] Z. K. Peng and F. L. Chu, "Application of the wavelet transform in machine condition monitoring and fault diagnostics: a review with bibliography," *Mechanical Systems and Signal Processing*, vol. 18, no. 2, pp. 199–221, 2004.

[8] S. Prabhakar, A. R. Mohanty, and A. S. Sekhar, "Application of discrete wavelet transform for detection of ball bearing race faults," *Tribology International*, vol. 35, no. 12, pp. 793–800, 2002.

[9] C. K. Sung, H. M. Tai, and C. W. Chen, "Locating defects of a gear system by the technique of wavelet transform," *Mechanism and Machine Theory*, vol. 35, no. 8, pp. 1169–1182, 2000.

[10] A. Djebala, N. Ouelaa, and N. Hamzaoui, "Detection of rolling bearing defects using discrete wavelet analysis," *Meccanica*, vol. 43, no. 3, pp. 339–348, 2007.

[11] H. Han, S. Cho, S. Kwon, and S.-B. Cho, "Fault diagnosis using improved complete ensemble empirical mode decomposition with adaptive noise and power-based intrinsic mode function selection algorithm," *Electronics*, vol. 7, no. 2, p. 16, 2018.

[12] H. Zheng, Z. Li, and X. Chen, "Gear fault diagnosis based on continuous wavelet transform," *Mechanical Systems and Signal Processing*, vol. 16, no. 2-3, pp. 447–457, 2002.

[13] J. Ben Ali, N. Fnaiech, L. Saidi, B. Chebel-Morello, and F. Fnaiech, "Application of empirical mode decomposition and artificial neural network for automatic bearing fault diagnosis based on vibration signals," *Applied Acoustics*, vol. 89, pp. 16–27, 2015.

[14] M. R. Castelino, H. S. Kumar, and G. S. Vijay, "Artificial neural network based vibration signal analysis of rotary machines-case studies," in *Proceedings International Conference on Emerging Trends in Engineering (ICETE-2014) @ NITTE*, pp. 211–218, London, UK, May 2014.

[15] J. Gai and Y. Hu, "Research on fault diagnosis based on singular value decomposition and Fuzzy neural network," *Shock and Vibration*, vol. 2018, Article ID 8218657, 7 pages, 2018.

[16] I. Ballo, *Skúšobné Otázky Pre Vibrodiagnostiku*, COPTD, Nitra, Slovakia, 2001.

[17] I. Ballo and M. Peteri, *Skúšobné Otázky Pre Vibrodiagnostiku 2, Nitra*, 2002, http://www.cmms.cz/uvod.html.

[18] O. Valent, M. Galád, and Ĺ. Kačmar, *Technická diagnostika 3*, Ustavování strojů, CMMS, Praha, Czech Republic, 2010.

[19] A. Panda, *Stanovenie Spôsobilosti Obrábacích Strojov, Strojárstvo 5/2000*, Media/ST s.r.o., Žilina, Slovakia, 2000.

[20] SKF Ložiska, a.s., Praha, *Ustavování hřídelů, Aplikační materiál FIXTUR LASER*, SKF Ložiska, a.s., Prague, Czech Republic, 2017.

[21] K. Juliš, V. Borůvka, and B. Fryml, *Základy Dynamického Vyvažování*, SNTL, Berlin, Germany, 1979.

[22] P. Baron, M. Kočiško, J. Dobránsky, M. Pollák, and M. Telišková, "Research and application of methods of technical diagnostics for the verification of the design node," *Measurement*, vol. 94, pp. 245–253, 2016.

[23] J. Piotrowski, *Shaft Alignment Handbook*, CRC Press Taylor and Francis Group, Boca Raton, FL, USA, 2007.

[24] G. Krolczyk, M. Gajek, and S. Legutko, "Predicting the tool life in the dry machining of duplex stainless steel," *Eksploatacja i Niezawodnosc-Maintenance and Reliability*, vol. 15, no. 1, pp. 62–65, 2013.

[25] G. Krolczyk, J. Krolczyk, S. Legutko, and A. Hunjet, "Effect of the disc processing technology on the vibration level of the chipper during operations process," *Technical Gazette*, vol. 21, no. 2, pp. 447–450, 2014.

[26] L. Šeremeta, *Podkladové Materiály k Ustavování*, LAMI KAPPA s.r.o., Teplice, Czech Republic, 2004.

[27] I. Kuric, M. Císar, V. Tlach, I. Zajačko, T. Gál, and D. Więcek, "Technical diagnostics at the department of automation and production systems," in *Proceedings of 2nd International Conference on Intelligent Systems in Production Engineering and Maintenance, ISPEM 2018*, vol. 835, pp. 474–484, Wroclaw, Poland, August 2019.